Chemosphere 307 (2022) 135805

Contents lists available at ScienceDirect

Chemosphere

journal homepage: www.elsevier.com/locate/chemosphere

Seawater intrusion induced cadmium activation via altering its distribution and transformation in paddy soil

Wenting Chi [a,b,c,1], Yang Yang [b,1], Ke Zhang [b], Pei Wang [b], Yanhong Du [b], Xiaomin Li [b,d,e], Yan Sun [b], Tongxu Liu [b,*], Fangbai Li [b]

[a] Guangzhou Institute of Geochemistry, Chinese Academy of Sciences, Guangzhou, 510640, PR China
[b] National-Regional Joint Engineering Research Center for Soil Pollution Control and Remediation in South China, Guangdong Key Laboratory of Integrated Agro-environmental Pollution Control and Management, Institute of Eco-environmental and Soil Sciences, Guangdong Academy of Sciences, Guangzhou, 510650, PR China
[c] University of Chinese Academy of Sciences, Beijing, 100049, PR China
[d] SCNU Environmental Research Institute, Guangdong Provincial Key Laboratory of Chemical Pollution and Environmental Safety & MOE Key Laboratory of Theoretical Chemistry of Environment, South China Normal University, Guangzhou 510006, PR China
[e] School of Environment, South China Normal University, Guangzhou 510006, PR China

HIGHLIGHTS

- High salinity promotes Cd dissolution from paddy soil.
- Cd competition and complexation dominated the release of Cd from soils.
- The pH was elevated with high salinity but the Cd availability increased.
- The effect of salt on redox process contributed to the remobilization of Cd.

GRAPHICAL ABSTRACT

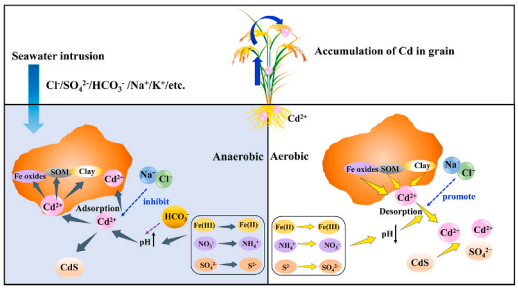

ARTICLE INFO

Handling editor. Yanzheng Gao

Keywords:
Cadmium
Salinity
Paddy soil
Kinetics

ABSTRACT

Seawater intrusion can cause environmental risks to paddy soils around estuaries, but the impacts on the availability of heavy metals are still unclear. River water and sea water were collected along the river of an estuary. A stirred-flow experiment was conducted to examine the Cd desorption behavior in Cd-contaminated paddy soil. While the pH increased with increasing salinity levels, more Cd was released with increasing salinity, suggesting that Cd competition by cations and complexation by anions, but not pH, dominated the release of Cd from soils. Moreover, paddy soil was incubated at different salinities under alternating redox conditions. The availability of Cd, as indicated by the diffusive gradients in thin film (DGT), became relatively high with increasing salinity levels during the initial anaerobic and later aerobic stages. The available Cd fractions substantially decreased under anaerobic condition, and then rapidly increased under aerobic condition. When oxygen was introduced into the system, Cd associated with organic matter and Fe–Mn oxides were released, and oxidative dissolution of Cd sulfides was observed, especially in the high salinity treatment. Seawater intrusion affects biogeochemical cycles and can promote rapid export of NH_4^+, Fe^{2+}, and SO_4^{2-} in paddy

* Corresponding author.
E-mail address: txliu@soil.gd.cn (T. Liu).
[1] Co-first authors: These authors contributed equally to this work.

https://doi.org/10.1016/j.chemosphere.2022.135805
Received 29 April 2022; Received in revised form 27 June 2022; Accepted 19 July 2022
Available online 30 July 2022

soils, especially in soils with high salinity. Our findings demonstrated that the high salinity content in paddy soil significantly enhanced the availability of Cd, especially during the drainage stage.

1. Introduction

Periodic tides and rising sea levels cause seawater intrusion into paddy fields (Reddy et al., 2017; Tully et al., 2019) located around estuaries, resulting in an increase in the salt content in soils and the consequent environmental risk (Guo et al., 2016). Increasing salinity may cause a delay in panicle emergence and flowering and a reduction in rice yield (Viet and Bharali, 2019). Moreover, the abundant cations and anions from seawater intrusion could influence the availability of heavy metals, especially cadmium (Cd), which is one of the most important elements due to its high mobility and toxicity (Wan et al., 2019; Wang et al., 2019). The major rice production area is located in southern China, including vast regions around the long coastline; however, the environmental risk of seawater intrusion to heavy metals has been ignored. Therefore, it is essential to clarify how and to what extent cations and anions in sea water affect Cd availability.

The main cations and anions in sea water included Na^+, K^+, Mg^{2+}, Cl^-, HCO_3^-, SO_4^{2-}, and so on (Steinmuller and Chambers, 2018). The complexation and adsorption of Cd are very important for Cd retention from the outer-to the inner sphere of soil surfaces, such as organic matter, clay minerals, metal oxides and so on (Hu et al., 2016; Zhang et al., 2018). Cations (e.g., Mg^{2+}) may compete with dissolved Cd^{2+} for limited adsorption sites (Loganathan et al., 2012), causing the desorption of Cd into the solution (Wang et al., 2013; Li et al., 2018). Being the most important anion in seawater, Cl^- can form complex with Cd as $CdCl^+$ and $CdCl_2^0$, both of which can be easily taken up by plants (Smolders and McLaughlin, 1996; López-Chuken and Young, 2010; Hu et al., 2016). Alkaline anion (HCO_3^-) can elevate the soil pH, which directly influences the equilibrium of Cd at the soil-water interface (Loganathan et al., 2012; Tavakkoli et al., 2015). A high pH was favorable for the adsorption process, which was conducive to the further immobilization of Cd. These cations and anions co-exist in sea water, and thus, there are two apparently contradictory processes: adsorption and desorption. Therefore, the dominant mechanisms that control Cd availability in paddy soil should be clarified.

In paddy fields, rice is usually cultivated under flooding condition because of its sensitivity to water shortages, and flooded paddy fields drain for two or three weeks before rice maturity (Wang et al., 2019). Many factors (e.g., water management, water stress, etc.) influence the promotion of rice growth and grain maturation, while water management by drainage significantly alters the redox conditions (Ondrasek, 2014; Pandey et al., 2014; Pan et al., 2016). Generally, oxygen is rapidly depleted from flooded paddy fields, and therefore, alternative electron acceptors (e.g., NO_3^-, SO_4^{2-}, and Fe/Mn oxides) are used to anaerobically metabolize organic substances (Kögel-Knabner et al., 2010; Chen et al., 2020). Large amounts of protons are consumed during the reduction of nitrate, sulfate, and Fe/Mn oxides, which leads to a significant increase in the pH of acidic paddy soils (Yuan et al., 2019; Yang et al., 2021). The availability of Cd significantly decreases during the flooding phase, which can be attributed to the strong adsorption induced by increasing soil pH, co-precipitation with anaerobically formed secondary Fe(III) oxides, and precipitation as Cd sulfides (Fulda et al., 2013; Suda and Makino, 2016; Wang et al., 2016a, 2019). After the drainage of the flooded paddy fields, large quantities of reducing substances (e.g., NH_4^+, S^{2-}, Fe(II), and Mn(II), etc.) are rapidly oxidized, and there is a corresponding release of protons (Grybos et al., 2009; Yu et al., 2016; He et al., 2019; Yang et al., 2021). The decrease in soil pH may significantly enhance desorption of Cd from soil surfaces. Moreover, the oxidation of Cd sulfides can contribute to the release of Cd into the solution (Fulda et al., 2013; Wang et al., 2019).

Although the effects of relatively high salinity (ionic strength of 200 mM) on Cd accumulation in rice have been studied (Yang et al., 2022), our understanding of the effects of relatively low salinity (ionic strength of 30 mM) on Cd speciation in paddy soil and Cd accumulation in rice grains are still limited. Salt-tolerant rice cultivars (sea rice) can produce nutrient-rich grains when grown in high salinity soils, but the accumulation of Cd in plant tissues is much higher than that in common rice varieties (Chen et al., 2017; Yang et al., 2019b). It has been reported that, in wetland soil under flooding condition, salinity significantly increase the content of exchangeable Cd in the soil and increases the mobility of Cd (Chu et al., 2015). Guo et al. (2016) reported a significant increase in Cd availability during flooding, or drainage cycles, incubated with seawater with 3.34% salinity (ionic strength of 552 mM). Generally, salinity levels with ionic strengths within 30 mM had no significant influence on rice yield (Tanji and Kielen, 2002). The relatively high salinity (ionic strength of 200 mM) significantly increased the concentration of Cd in rice grains, while the soil pot experiment was conducted under the condition of continuous flooding during rice growth (Yang et al., 2022). However, whether and to what extent Cd availability changes in relatively low salinity (ionic strength of 30 mM) paddy soils during alternating redox conditions is still unclear.

In this study, we investigated Cd desorption and the dynamics of Cd speciation under alternating redox conditions with different salinity levels. The aims of this study were to (i) examine the impacts of sea water on Cd speciation and Fe/N/S/C cycling, (ii) clarify the dominant factors controlling salt-induced Cd desorption behaviors, and (iii) quantitatively assess the effects of key redox reactions in sea water on the dynamics of Cd fractions.

2. Materials and methods

2.1. Soil samples and sea water

Cd-contaminated paddy soil (Ultisol) was collected from Shaoguan City (24°38′19″ N, 113°35′22″ E) in Guangdong Province, China. Soil samples were air-dried and sieved (2 mm mesh size) for further experimentation. The soil characteristics analyzed included pH, carbonate ($CaCO_3$), clay, total organic carbon (TOC), cation exchange capacity (CEC), specific surface area (SSA), amorphous Fe/Mn oxides (Ox–Fe and Ox–Mn), and total content of Fe, Mn, and Cd. The physical and chemical properties of the paddy soil are presented in the Appendix A (Table S1).

Sea water with different salinity levels was collected along the Pearl River to the estuary in Jiangmen, Guangdong Province, China. The content of cations (Na^+, K^+, Ca^{2+}, and Mg^{2+}), concentration of anions (NO_3^-, SO_4^{2-}, and Cl^-), HCO_3^- content, and ionic strength of the water are

Table 1
The characterization of sea water collected from different areas around the estuary.

Parameters	Different salinity levels		
	Control	Low salinity	High salinity
pH	6.23	6.86	7.25
Na^+ (mM)	0.73	5.83	13.59
Ca^{2+} (mM)	0.68	0.86	1.72
Mg^{2+} (mM)	0.20	0.92	3.22
K^+ (mM)	0.15	0.28	1.46
Cl^- (mM)	1.95	7.40	23.27
SO_4^{2-} (mM)	0.10	0.57	2.04
HCO_3^- (mM)	0.13	0.11	0.21
NO_3^- (mM)	0.02	0.06	0.24
Ionic strength (mM) [a]	3.42	11.20	31.20

[a] Ionic strength was calculated by using Visual MINTEQ 3.1.

summarized in Table 1.

2.2. The experiments of desorption kinetics

A stirred-flow kinetic method was used to investigate the desorption kinetics of Cd from paddy soil sample (Tian et al., 2017; Liu et al., 2019). Briefly, a 0.6 g uncultured dry soil sample and the magnetic agitator were placed in an 8.5 cm^3 reactor with three different salinities of sea water, and the stirring rate was set at 500 r min^{-1}. Three different salinities of sea water were pumped into the reactor at a constant flow rate (1 mL min^{-1}). The soil was retained in the reactor using a water phase filtration membrane (0.22 μm). The stirring flow was operated continuously for 4 h, and the outflow was automatically collected every 6 min.

2.3. The soil incubation experiments

Periodic flooding and drainage conditions were simulated using the microcosm method to investigate the dynamics of heavy metals in paddy soils (Fulda et al., 2013; Wang et al., 2019; Yang et al., 2021). The soil incubation experiment simulated the occurrence of typical flooding/drainage paddy field and followed the microcosm method as described by Wang et al. (2019). Since the drainage period generally occurs 2–3 weeks before rice maturity, the soils were anaerobic incubated for 40 d, then reoxygenated and aerated for 20 d. Briefly, 5 g aliquots of soil were placed into 50 mL penicillin bottles containing 25 mL of sea water. The ionic strengths of the water were 3.42 mM (control), 11.20 mM (low salinity) and 31.20 mM (high salinity) (Table 1). The bottles were placed in an anaerobic chamber (H_2/N_2 (2/98, v/v), Plas-Labs, U.S.A.) to replace the headspace gas with N_2. During the anaerobic stages (0, 5, 20, and 40 d) and aerobic stages (2, 7, 15, and 20 d), three replicates of incubation bottles were destructively sampled for chemical analysis.

Soil pH, Eh, the contents of Cd^{2+}, NH_4^+, NO_3^-, SO_4^{2-}, Fe^{2+}, amorphous Fe(III), and reduced Fe(II), and dissolved organic matter (DOC) were analyzed. The available Cd concentration was estimated using the diffusive gradients in thin film (DGT) technique, which can assess the transport of metals from soil to solution in paddy fields (Xiao et al., 2020). To further evaluate Cd speciation, a seven-step sequential extraction method was performed, according to Krishnamurti and Naidu (2003). Briefly, (1) dissolved Cd (F0) was obtained from the filtered supernatants; (2) exchangeable Cd (F1) was extracted by $MgCl_2$ (1 M, pH = 7, shake 1 h, 25 °C) from a 2 g wet soil sample; (3) carbonate bound Cd (F2) was extracted with NaOAc (1 M, pH = 5, shake 1 h, 25 °C); (4) fulvic-complexed Cd (F3) was extracted with $Na_4P_2O_7$ (0.1 M, pH = 1, shake 2 h, 25 °C); (5) humic-complexed Cd (F4) was extracted with $Na_4P_2O_7$ (0.1 M, pH = 10, shake 2 h, 25 °C); (6) Fe–Mn oxides-bound Cd (F5) was extracted with $NH_2OH{\cdot}HCl$ (0.04 M, 25% HOAc (v/v), shake 6 h, 96 °C); (7) sulfides-bound Cd (F6) was extracted with 30% H_2O_2 (pH 2.0, shake 5 h, 85 °C) and NH_4OAc (3.2 M, 20% HNO_3 (v/v), shake 0.5 h, 25 °C); and (8) residual Cd (F7) was digested using HNO_3–$HClO_4$–HF (15: 2: 2, v/v/v). For digestion soil samples, quality assurance and quality control were performed for blank and standard for every nine soil samples using duplicates, and certified standard reference materials (GBW(E)07429 for soil Cd) were obtained from the National Research Center for Standards in China. Cd recovery ranged from 90% to 103% for the digestion soil samples. The recovery of Cd (sum of fractions/total Cd × 100%) ranged from 98 to 105%. The surface site concentration (H_s) in the different treatments during anaerobic stage (0, 5, 20, and 40 d) and aerobic stage (2, 7, 15, and 20 d) were obtained using the Gran plot method by conducting continuous potentiometric titration experiments (905 Titrando, Metrohm, Switzerland) (Yang et al., 2019a, 2020). The H_s was obtained by a Gran plot, and the detailed methods is presented in Appendix A (Text 1).

2.4. Methods of chemical analysis

For the soil sample, the pH was determined in a 0.01 M $CaCl_2$ solution at a 1: 2.5 ratio using a pH/Eh meter (Seven-Compact S220, Mettler-Toledo, Switzerland). The carbonate ($CaCO_3$) content was measured using the neutralization titration method (Lu, 2000), the clay content was determined using the pipette method (Abdulaha Al Baquy et al., 2018), the soil samples were digested with HNO_3–$HClO_4$–HF (Lambrechts et al., 2011), and the concentrations of Fe and Mn in the digests were measured using inductively coupled plasma-optical emission spectroscopy (ICP-OES, Optima 8000, PerkinElmer, U.S.A.). The total organic carbon (TOC) was measured using a TOC analyzer (TOC-L CPH, Shimadzu, Japan), the cation exchange capacity (CEC) was determined using the ammonium acetate method (Curtin and Trolove, 2013). The specific surface area (SSA) was determined by the ethylene glycol monoethyl ether method (Cerato and Lutenegger, 2002). The Cd content of the aqueous solution was determined using graphite furnace atomic absorption spectrometer (GF-AAS) (PinAAcle 900, PerkinElmer, USA), and the Cd, Fe, and Mn contents in the solution were determined using ICP-OES.

For soil incubation, the soluble NH_4^+ was determined using the colorimetric method at 420 nm using a UV–vis spectrophotometer (TU-1950, Persee, China) (Zhang et al., 2012). Dissolved NO_3^- and SO_4^{2-} were analyzed using ion-exchange chromatography (IC) (ICS-600, DioneX, U.S.A.), and dissolved Fe^{2+} was determined using the o-phenanthroline colorimetric method using a UV–vis spectrophotometer (Lu, 2000). HCl (0.5 M) was used to extract amorphous Fe(III) and reduced Fe(II) species (Heron et al., 1994). The total extracted Fe (T-Fe_{HCl}) in the filtrate was measured using ICP-OES. The $Fe(II)_{HCl}$ concentration was determined using the colorimetric method ($Fe(III)_{HCl}$ = T-Fe_{HCl} – $Fe(II)_{HCl}$). The dissolved organic carbon (DOC) was measured using a TOC analyzer (TOC-L CPH, Shimadzu, Japan). Cd availability was assessed using standard piston DGT devices (DGT Research, Lancaster, UK) containing a Chelex-100 (Bio-Rad, USA), according to the literature (Ding et al., 2015; Wang et al., 2016b; Yang et al., 2021).

2.5. Statistical analysis

The statistical analysis was performed using the SPSS software (version 22.0, IBM Corporation, Armonk, New York, U.S.A.). The dynamics of Cd transformation were further analyzed by first-order kinetics using the KinTek Explorer 8.0 software (Johnson et al., 2009; Yang et al., 2021). The best fit of the rate constant and the corresponding upper and lower bounds were obtained using the chi^2 test with a threshold of 0.95 (Chen et al., 2021).

3. Results and discussion

3.1. Kinetics of Cd release from soil in different salinity water

As shown in Fig. 1a, the solution pH increased during the stir-flow experiment, because the initial pH values of the sea water were 6.23, 6.86, and 7.25 (Yang et al., 2020). After 100 min, the solution pH remained unchanged, as the acidic ions (e.g., H^+, Al^{3+} and so on) were almost depleted in the system (Xu et al., 2012; Jiang et al., 2018). Generally, increasing pH can enhance Cd adsorption on soil surfaces (Liu et al., 2018), but results in Fig. 1b show that the concentration of dissolved Cd was much higher under the high salinity treatment than that under the low salinity and control treatments, especially during the initial stage (Fig. 1b). This indicates that the high salinity levels in the water considerably enhanced the release of Cd from the soil. After the rapid release of Cd during the first 60 min, the dissolved Cd content gradually decreased to nearly zero at the outflow. As shown in Fig. 1b, the first-order rate constants were in the following order: high salinity ≫ low salinity > control, demonstrating that increasing salinity levels substantially enhanced the desorption of Cd, especially under the high

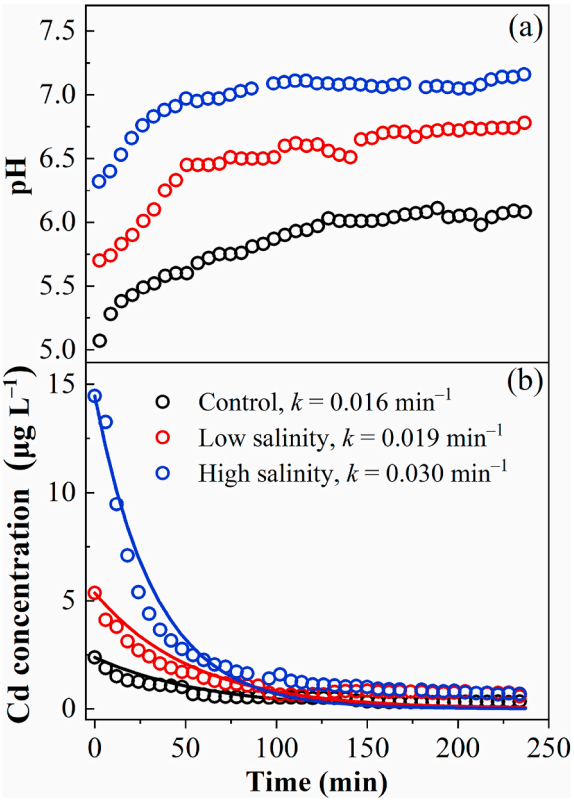

Fig. 1. The kinetics of pH (a) and the release of Cd (b) in the stirred–flow system. The solid lines represent the model fit values. Control (3.42 mM), low salinity (11.20 mM), and high salinity (31.20 mM) represent three salinity levels of water.

salinity treatment. This indicated that competition and complexation-induced Cd release, rather than the pH-dependent adsorption process, was the dominant process controlling Cd availability. First, this may be attributed to the strong ion exchange capacities of cations (Na^+, K^+, Ca^{2+}, and Mg^{2+}) that cause higher Cd release (Esfandiar et al., 2022). Elevated salinity promotes the release of exchangeable metals from the particle surface to the diffuse double-layer as cations compete for adsorption sites (Behbahani et al., 2021). Second, Cd^{2+} can remain in aqueous solution by forming water-soluble complexes (e.g., $CdCl_n^{2-n}$ and $CdSO_4$, etc.) with Cl^- and SO_4^{2-}, which promotes the desorption of Cd in soil (Ondrasek et al., 2020, 2022; Chi et al., 2022). In saline irrigation water soil (ionic strength of 30 mM) up to 80% and 2% of the inorganic Cd in soil solution was present as chloride and sulfate complexes, respectively (Weggler et al., 2004).

3.2. Dynamics of Cd fractions under alternating redox conditions

The results in Fig. 2 show that there was a significant difference in the available Cd determined by DGT (Cd_{DGT}) at the initial stage (0 d). The Cd_{DGT} under the high salinity treatment (8.45 μg L^{-1}) was much higher than that under the low salinity (5.39 μg L^{-1}) and control (4.89 μg L^{-1}) treatments. After 5 d of anaerobic incubation, the Cd_{DGT} of the three treatments rapidly declined to nearly zero and remained unchanged until the end of the anaerobic stage. During the last 5 d of the aerobic stage, the Cd_{DGT} increased substantially in the order of high salinity ≫ low salinity > control. A significant increase in the Cd_{DGT} was also observed after adding 120 mM of NaCl (Oporto et al., 2009), which might be due to the contribution of the $CdCl_n^{2-n}$ complex to the DGT flux. Some researchers proved that the measurement of Cd by DGT using Chelex as a resin binding agent is independent of ionic strength (Zhang

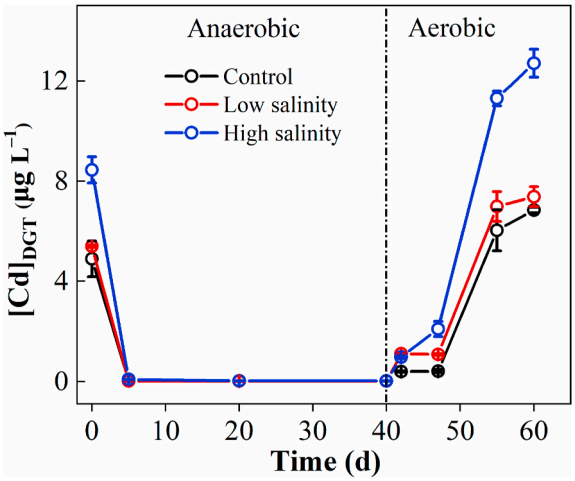

Fig. 2. Available Cd concentration measured by diffusive gradients in a thin film (DGT) under different salinity levels. Control (3.42 mM), low salinity (11.20 mM), and high salinity (31.20 mM) represent three salinity levels of water.

and Davison, 1995). Others argued that the decrease in metal accumulation with decreasing ionic strength is due to electrostatic repulsion effects and a decrease in ligand-assisted dissociation (Puy et al., 2014). Dissolved unstable complexes (such as $CdCl_n^{2-n}$) enhance the diffusive supply of Cd^{2+} through dissociation of the complexes in the DGT diffusion layer, thus improving the availability of Cd (Oporto et al., 2009). The high salinity levels in the sea water considerably promoted the release of Cd_{DGT} and Cd desorption from the soil (Figs. 1b and 2). The result trend of the Cd_{DGT} was consistent with that of Cd desorption characteristics, indicating that Cd was activated by the high-salinity water under the aerobic condition.

The results in Fig. 3a–h shows the temporal changes in the Cd fractions (F0–F7) in under salinity levels. Under anaerobic condition, the dissolved Cd and exchangeable Cd (F0 and F1) rapidly declined, and a slight decrease was also observed for carbonate bound Cd (F2). The fulvic- and humic-complexed Cd (F3 and F4), Fe–Mn oxides-bound Cd (F5) and sulfides-bound Cd (F6) greatly increased. The highest dissolved Cd was observed during the initial anaerobic stage (0 d) under the high salinity treatment, followed by the low salinity and control treatments. There was no significant difference between the Cd fractions of F1 and F2 ($P > 0.05$) under anaerobic condition. The Cd fractions in F3, F4 and F5 were relatively high in control treatment, which reached the significant level on 20 and 40 d for F3 and F5, and 5 d for F4 ($P < 0.05$). The Cd fraction of F6 was relatively high under the high salinity treatment after 5 d of anaerobic incubation ($P < 0.05$). After aeration, the Cd fractions of F0, F1, and F2 increased considerably. The dissolved Cd (F0) was significantly higher under the high salinity treatment than that under the control and low salinity treatments during aerobic incubation at 47, 55, and 60 d ($P < 0.05$). Although relatively high F1 and F2 contents were found under the high salinity and low salinity treatments, a significant level was reached at 55 d for F1 and 60 d for F2. Moreover, the Cd fractions of F3–F6 rapidly decreased during the first 7 d of the aerobic stage, especially under the high salinity treatment. Residual Cd (F7) remained almost constant during the incubation period, suggesting that alternating redox conditions or different salinity levels had little effect on Cd transformation for the residual fraction. The dissolved, exchangeable, and carbonate bound Cd (F0, F1, and F2) can be considered easily mobile Cd (Fulda et al., 2013). Therefore, the high content of easily mobile Cd under the high salinity treatment indicated its relatively high Cd availability under aerobic condition, which was consistent with the results for the Cd_{DGT}.

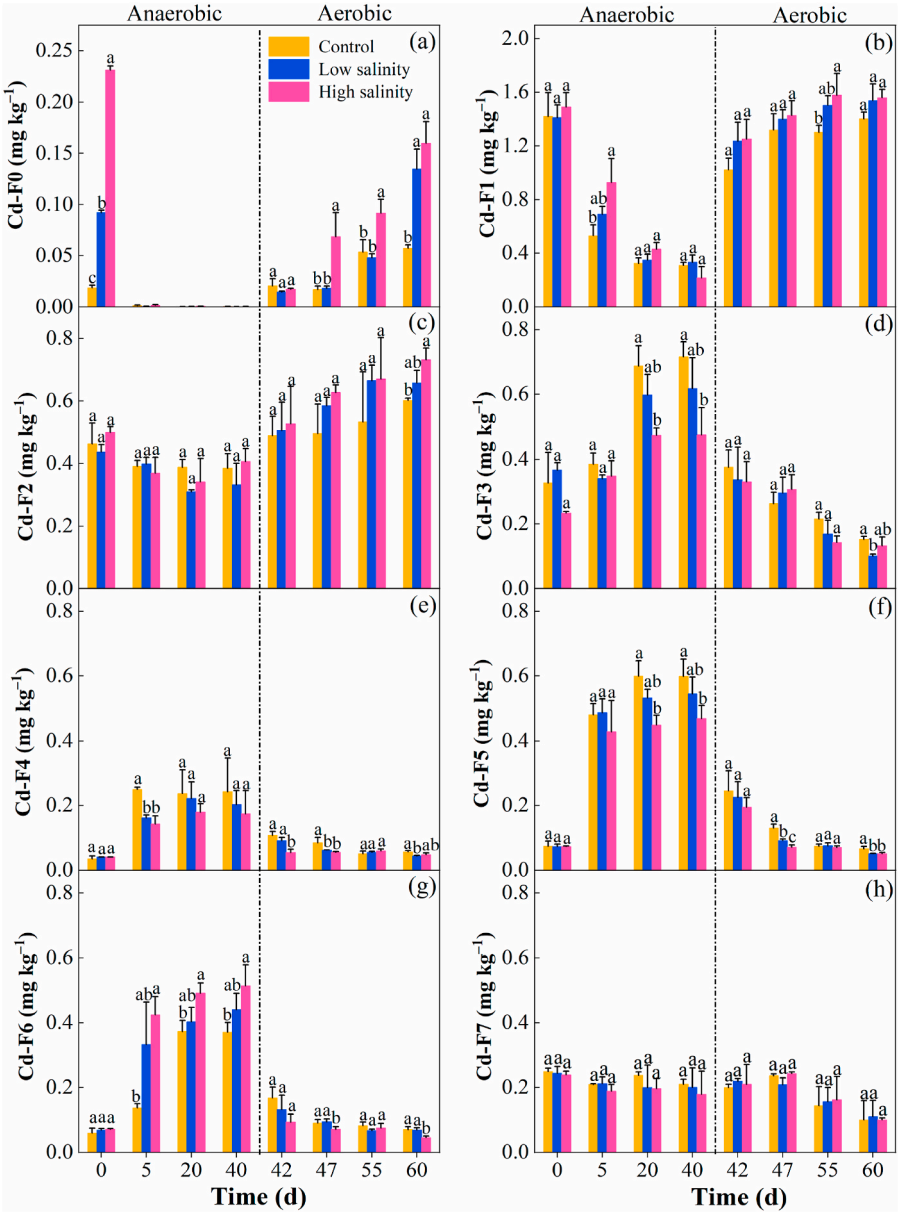

Fig. 3. Changes in Cd fractions (F0–F7) determined by chemical extraction under different salinity levels. F0: Dissolved Cd; F1: Exchangeable Cd; F2: Carbonate bound Cd; F3: Fulvic-complexed Cd; F4: Humic-complexed Cd, F5: Fe–Mn oxides-bound Cd; F6: Sulfides-bound Cd; F7: Residual Cd. Different letters in different treatments indicate significant differences at $P < 0.05$. Control (3.42 mM), low salinity (11.20 mM), and high salinity (31.20 mM) represent three salinity levels of water.

3.3. Changes in chemical properties

As shown in Fig. 4a and b, the soil pH under the three salinity levels rapidly increased from 5.0 to 6.6, while the Eh dramatically dropped from 330 mV to −233 mV after 5 d of anaerobic incubation, which may be attributed to the anaerobic fermentation of organic matter using alternative electron acceptors, including SO_4^{2-}, NO_3^-, and Fe(III) oxides, etc. (Kögel-Knabner et al., 2010; He et al., 2015). The reduction sequence of inorganic substances in soil was arranged from high to low in Eh, mainly NO_3^-, Fe(III) oxides and SO_4^{2-}, etc (de Livera et al., 2011; Hussain et al., 2021), and the anaerobic reactions were present as below.

$$\frac{1}{8}NO_3^- + \frac{5}{4}H^+ + e^- = \frac{1}{8}NH_4^+ + \frac{3}{8}H_2O \quad (1)$$

$$Fe(OH)_3 + 3H^+ + e^- = Fe^{2+} + 3H_2O \quad (2)$$

$$\frac{1}{8}SO_4^{2-} + \frac{5}{4}H^+ + e^- = \frac{1}{8}H_2S + \frac{1}{2}H_2O \quad (3)$$

The SO_4^{2-}, NO_3^-, and $Fe(III)_{HCl}$ concentrations (Fig. 4c–e) decreased, while the dissolved Fe(II) and $Fe(II)_{HCl}$ contents increased (Fig. 4f and g). Moreover, the release of dissolved organic matter (DOC) and NH_4^+ may be due to the breakdown of soil aggregation, which was induced by the reductive dissolution of Fe(III) oxides as the dominant cementing agents in paddy soils (Fig. 4h and i) (Grybos et al., 2009; Lu et al., 2014). The breakdown of soil aggregates also increased the surface site concentration (H_s) and potentially facilitated the retention of Cd (Fig. 4j) (Yang et al., 2021).

Although the pH of the water under varying salinities was ranked in the order of high salinity > low salinity > control (Table 1), no significant change was observed in soil pH during the anaerobic stage, indicating that the soil buffering ability had the dominant effect on the soil

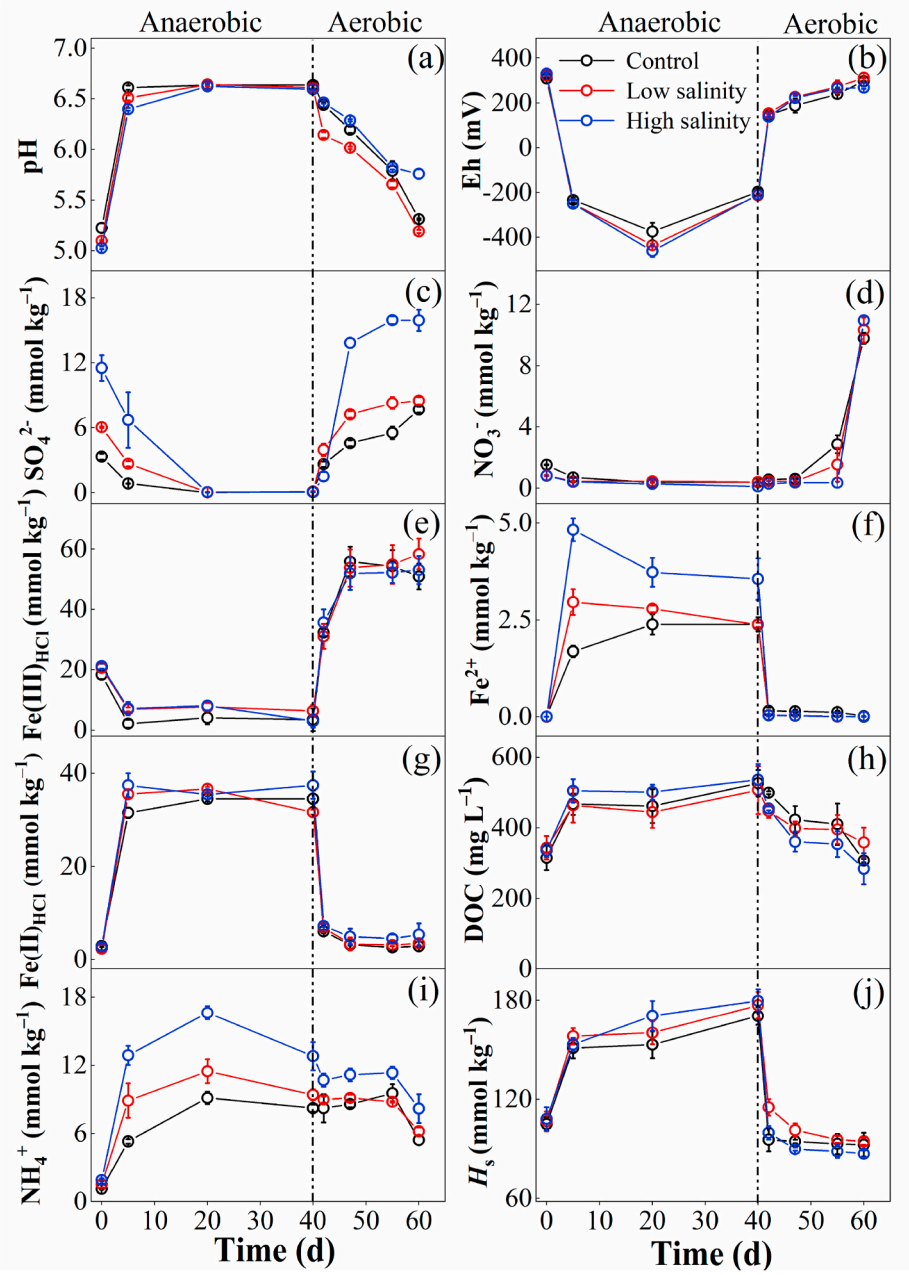

Fig. 4. Changes in pH (a), Eh (b), SO_4^{2-} (c), NO_3^- (d), $Fe(III)_{HCl}$ (e), Fe^{2+} (f), $Fe(II)_{HCl}$ (g), DOC (h), NH_4^+ (i) and surface site concentration (H_s) (j) under different salinity levels. Control (3.42 mM), low salinity (11.20 mM), and high salinity (31.20 mM) represent three salinity levels of water.

pH (Yang et al., 2020). During the initial 5 d of the anaerobic stage, the rapid decrease in dissolved Cd may be due to the enhancement of Cd adsorption on negatively charged soil surfaces due to the elevated pH (Figs. 3a and 4a) (Yang et al., 2019a). Specifically, high pH can facilitate slow migration of Cd from the outer to the inner sphere, including the surface of soil organic matter and Fe–Mn oxides (Zhang et al., 2018). Therefore, long-term incubation can effectively enhance the retention of Cd by organic matter and Fe–Mn oxides (F3–F5) from easily mobile fractions (F1 and F2) (Fig. 3b–f). Under the high salinity treatment, large amounts of cations (e.g., Na^+, Ca^{2+}, Mg^{2+}, etc.) may compete for limited binding sites, resulting in an increase in dissolved Fe^{2+} and NH_4^+ (Fig. 4f and i). Therefore, the low contents of F3–F5 under the high salinity treatment might be due to competition from cations for migration into the inner sphere of soil surfaces (Zhang et al., 2018). In addition, the amount of sulfides-bound Cd was correlated with the sulfate content (control < low salinity < high salinity) (Figs. 3g and 4c), indicating that sulfate contributed to the formation of sulfides-bound Cd to some extent under anaerobic condition (Furuya et al., 2016).

After oxygen was re–introduced into the system under aerobic condition, the Eh rapidly increased to 154 mV (42 d, Fig. 4b), indicating the fast establishment of oxidizing condition. The oxidation of large quantities of reducing substances (e.g., NH_4^+, Fe(II), sulfides, etc.) occurred with a concomitant release of protons, resulting in a sharp decrease in soil pH (Fig. 4a) (Yang et al., 2021), and the contents of NO_3^-, $Fe(III)_{HCl}$, and SO_4^{2-} increased quickly. The above aerobic reactions were shown below.

$$NH_4^+ + 2O_2 = NO_3^- + 2H^+ + H_2O \quad (4)$$

$$Fe^{2+} + \frac{1}{4}O_2 + \frac{5}{2}H_2O = Fe(OH)_3 + 2H^+ \quad (5)$$

$$\frac{1}{8}H_2S + \frac{1}{4}O_2 = \frac{1}{8}SO_4^{2-} + \frac{1}{4}H^+ \quad (6)$$

The decrease in DOC might be due to the re–adsorption of DOC on positively charged soil surfaces because of the decrease in soil pH (Grybos et al., 2009). The results showed that H_s values increased from 107 to 179 mmol kg^{-1} during the anaerobic stage, while it decreased to 90 mmol kg^{-1} during the aerobic stage, and no significant changes were observed for the three salinity treatments. Moreover, there was a dramatic decrease in the surface site concentration because the oxidation of Fe(II) and the new formation of Fe(III) oxides can not only adsorb negatively charged ions (such as DOC), but can also enhance the re–aggregation of soil colloids (Lu et al., 2014; Yang et al., 2021; Song et al., 2022; Zhang et al., 2023).

During the aerobic stage, the soil pH was ranked in the order: low salinity < control < high salinity (Fig. 4a), but a relatively high dissolved Cd content was observed under the high salinity treatment (Fig. 3a) because the salinity levels, rather than soil pH, dominated the distribution of Cd at the soil-water interface (Loganathan et al., 2012; Li et al., 2018). Moreover, the high cation and anion contents under the low salinity and high salinity treatments may be conducive to the release of Cd from Fe–Mn oxides and organic matter, resulting in relatively high contents of F1 and F2. Although a high sulfate content can enhance the retention of Cd by precipitation with sulfides under the high salinity treatment during the anaerobic stage, the Cd sulfides were readily oxidized after aeration of the systems, resulting in the release of dissolved Cd (Wang et al., 2019).

3.4. Modeling evaluation of Cd transformation under different salinity

Based on previous results, the easily available Cd fractions (F0, F1 and F2) substantially decreased during the anaerobic stage, and then were remobilized after aeration of the systems, indicating the reversibility of Cd fractions during alternating redox conditions. Given that the residual Cd remained constant in the incubation experiment, the change in residual Cd was not considered in the kinetic model. Therefore, the transformation of Cd fractions should be roughly divided into three processes: (i) immobilization by organic matter (F3 and F4) (Reaction 7, R7), (ii) retention by Fe–Mn oxides (R8), and (iii) precipitation with sulfides (R9).

$$Cd_{F0+F1+F2} \leftrightarrow Cd_{F3+F4} \quad k_1 \quad (7)$$

$$Cd_{F0+F1+F2} \leftrightarrow Cd_{F5} \quad k_2 \quad (8)$$

$$Cd_{F0+F1+F2} \leftrightarrow Cd_{F6} \quad k_3 \quad (9)$$

To further evaluate the effects of salinity level on the transformation of Cd fractions, a kinetic model was established based on the key reactions for Cd transformation as R7-R9 (Yang et al., 2021). The best-fit values of the rate constants were obtained (Table 2, Fig. S2) and the fitting curves matched well with the Cd fractions under different salinity levels (Fig. S3). The k_+ and k_- represent the forward and backward rate constants, respectively. The transformation of the Cd fractions is also presented in Fig. 5, based on the modeling results. During the anaerobic stage, the rate constants k_{+1} and k_{+2} were higher under the control and low salinity treatments than that under the high salinity treatment, whereas k_{+3} was higher under the low salinity and high salinity treatments than that under the control treatment (Table 2). After aeration of the system, the rate constants k_{-1} and k_{-2} were slightly higher under the high salinity treatment than those under the low salinity and control treatments, and the highest k_{-3} value was observed under the high salinity treatment. As seen in Fig. 5, the modeling results clearly show that increasing salinity levels under anaerobic condition inhibited the immobilization of Cd by organic matter and Fe–Mn oxides, but enhanced the precipitation of Cd sulfides. During the aerobic stage, remobilization of Cd from organic matter and Fe–Mn oxides was substantially accelerated at high salinity levels, and the high content of Cd sulfides formed during the anaerobic stage was oxidatively dissolved. Our findings demonstrated that the availability of Cd can be greatly enhanced during the anaerobic and aerobic stages in a high salinity system.

Table 2
The rate constants (d^{-1}) of Cd transformation for three treatments under alternating redox conditions.

Treatments	Anaerobic			Aerobic		
Control	k_{+1} = 0.021	k_{+2} = 0.021	k_{+3} = 0.010	k_{-1} = 0.09	k_{-2} = 0.18	k_{-3} = 0.21
Low salinity	k_{+1} = 0.017	k_{+2} = 0.019	k_{+3} = 0.014	k_{-1} = 0.10	k_{-2} = 0.17	k_{-3} = 0.17
High salinity	k_{+1} = 0.014	k_{+2} = 0.011	k_{+3} = 0.014	k_{-1} = 0.11	k_{-2} = 0.22	k_{-3} = 0.92

The k_+ and k_- represent the forward and backward rate constants, respectively.

3.5. Environmental implications

Understanding the impacts of coastal seawater intrusion on heavy metals, biogeochemical processes, and plant relationships is important for assessing the changes in soil wetland systems and food security strategies in rice fields. As seawater intrusion intensifies and soil salinity increases, Cd becomes more susceptible to competitive exchange, complex formation, and desorption. In the present study, we provided evidence that the Cd desorption process caused by competition and complexation had a substantial effect on Cd availability under high salinity rather than pH. Seawater intrusion into freshwater wetlands increases sulfate availability (Steinmuller and Chambers, 2018). The increase in easily mobile Cd dominated the high Cd availability, and the rapid dissolution of sulfides-bound Cd over a short drainage period may also improve Cd solubility and plant availability (Fig. 3g). It is worth noting that 80% of Cd in rice seeds is accumulated during the filling period of rice growth, which usually coincides with preharvest soil drainage. Consequently, the Cd content in the rice may exceed the safety threshold for Cd in field trials (Inahara et al., 2007; Wang et al., 2019). Salt-tolerant rice cultivars (sea rice) have become a popular research topic because of their high yield in saline soils; however, the problem of Cd accumulation in rice has been neglected (Chen et al., 2017). Salinity in soil increase the Cd availability by the formation of $CdCl_n^{2-n}$ complexes (Ondrasek et al., 2020), thereby aggravating the Cd toxicity to the plants, as the salinity and Cd stress generally decreased the root length, plant height, panicle weight, and growth rate in plants (Thanh and Bharali, 2019; Yang et al., 2022). Combined with the results of the present research, valuable information is given on soil cadmium availability as an indication of the potential risk due to increased uptake of Cd by crops under saline conditions, particularly in the presence of Cl^-, enhanced Cd uptake may be a common trend for many edible crops. For example, increased Cd accumulation under high salinity exposure was found also in different biota, e.g., in radish cultivars (Ondrasek et al., 2020), lettuce (Ondrasek et al., 2021), and strawberry fruits (Ondrasek et al., 2022). The Cd accumulation by plants may be influenced by the salinity, water management, water stress, and plant species, etc (Pandey et al., 2014; Pan et al., 2016; Yang et al., 2022). Therefore, the risks should be fully considered for management strategies such as alternating wet and dry periods overlaid with soil salinity, as salinity promotes the bioavailability of Cd during short drainage cycles and in rice crops. Finally, the selection of rice cultivars with low Cd accumulation characteristics in highly saline soils could be an alternative for alleviating Cd toxicity in rice (Yang et al., 2019b). Additional work is however required to accurately investigate the Cd accumulation capacity of rice exposed to salinity under pot experiment and field conditions.

4. Conclusions

In this study, the effects of different salinity levels on Cd desorption

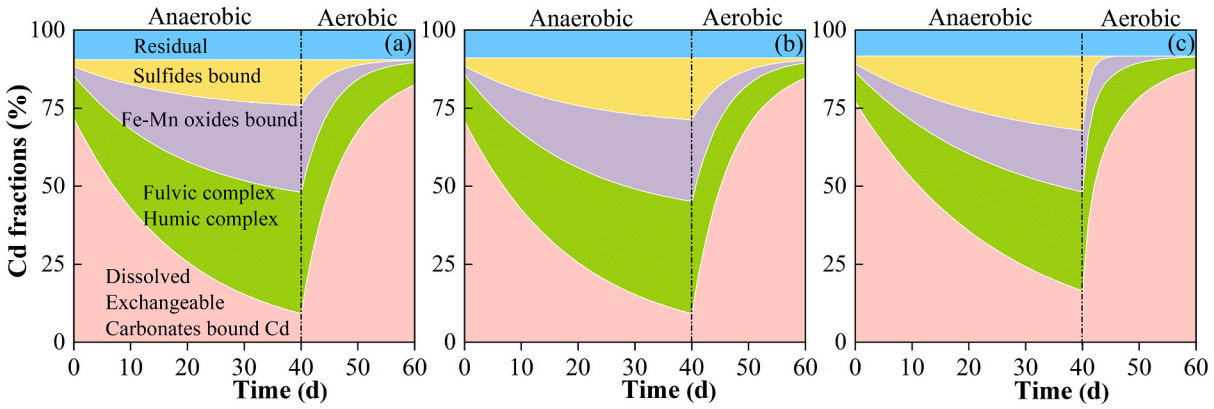

Fig. 5. The transformation of Cd fractions during anaerobic and aerobic stages under different salinity levels. (a) Control (3.42 mM), (b) low salinity (11.20 mM), and (c) high salinity (31.20 mM) represent three salinity levels of water.

and Cd_{DGT} were evaluated, and the dynamics of Cd fractions were investigated under anaerobic and aerobic conditions. Although soil pH increased with increasing salinity, Cd desorption was significantly enhanced due to competition from cations and complexation by anions. In the case of high salinity, dissolved unstable complexes (such as $CdCl_n^{2-n}$) may contribute to the Cd_{DGT} contribution. Moreover, the retention of Cd by organic matter and Fe–Mn oxides was also inhibited by salinity levels, while the precipitation of Cd sulfides may be facilitated by the high sulfate content in saline water. However, Cd sulfides were readily oxidized after aeration in the system, and the amounts of cations and anions in the relatively high-salinity water could further enhance the remobilization of Cd from organic matter and Fe–Mn oxides. Ionic replacement resulting from an increase in salinity probably caused the desorption of cations (e.g., NH_4^+ and Fe^{2+}) from the paddy soil, and the magnitude of this process increased with salinity. Paddy soils are vulnerable to seawater intrusion, which may alter soil biogeochemical processes, lead to the Cd release, and contribute to soil pollution. This study demonstrated the role of cations and anions in seawater in controlling Cd availability under alternating redox condition. Especially during the aerobic stage, high salinity substantially enhanced Cd remobilization, which may increase the extent of Cd accumulation in rice grains. This study provided a new insight into the impact of seawater intrusion on heavy metal pollution and risks and can be used to guide soil remediation in coastal environments.

Credit author statement

Wenting Chi: Validation, Formal analysis and Writing – Original Draft. **Yang Yang**: Methodology, Formal analysis and Writing – Review & Editing. **Ke Zhang**: Investigation and Resources. **Pei Wang**: Methodology. **Yanhong Du**: Resources. **Xiaomin Li**: Supervision and Project administration. **Tongxu Liu**: Conceptualization, Supervision and Funding acquisition. **Yan Sun**: Investigation. **Fangbai Li**: Project administration.

Declaration of competing interest

The authors declare that they have no known competing financial interests or personal relationships that could have appeared to influence the work reported in this paper.

Data availability

The authors are unable or have chosen not to specify which data has been used.

Acknowledgements

The work was funded by the National Natural Science Foundation of China (No. 42030702), China Postdoctoral Science Foundation (Nos. 2021M700888, 2021M701561), Guangdong Foundation for Program of Science and Technology Research (Grant No. 2019B121201004), Guangdong Basic and Applied Basic Reuter Foundation (No. 2019A1515011033).

Appendix A. Supplementary data

Supplementary data to this article can be found online at https://doi.org/10.1016/j.chemosphere.2022.135805.

References

Abdulaha Al Baquy, M., Li, J.Y., Jiang, J., Mehmood, K., Shi, R.Y., Xu, R.K., 2018. Critical pH and exchangeable Al of four acidic soils derived from different parent materials for maize crops. J. Soils Sediments 18, 1490–1499.

Behbahani, A., Ryan, R.J., McKenzie, E.R., 2021. Impacts of salinity on the dynamics of fine particles and their associated metals during stormwater management. Sci. Total Environ. 777, 146135.

Chi, W., Yang, Y., Liu, T., Sun, Y., Du, Y., Qin, H., Li, X., 2022. Effects of water salinity on cadmium availability at soil–water interface: implication for salt water intrusion. Environ. Sci. Pollut. Res. 1–12.

Chen, C., Hall, S.J., Coward, E., Thompson, A., 2020. Iron-mediated organic matter decomposition in humid soils can counteract protection. Nat. Commun. 11.

Chen, G., Zhao, W., Yang, Y., Chen, D., Wang, Y., Li, F., Zhao, Z., Cao, F., Liu, T., 2021. Chemodenitrification by Fe(II) and nitrite: effects of temperature and dual N-O isotope fractionation. Chem. Geol. 575, 120258.

Cerato, A.B., Lutenegger, A.J., 2002. Determination of surface area of fine-grained soils by the ethylene (EGME) method. Geotech. Test J. 25, 315–321.

Chen, R., Cheng, Y., Han, S., Van Handel, B., Dong, L., Li, X., Xie, X., 2017. Whole genome sequencing and comparative transcriptome analysis of a novel seawater adapted, salt-resistant rice cultivar-sea rice 86. BMC Genom. 18, 655.

Chu, B., Chen, X., Li, Q., Yang, Y., Mei, X., He, B., Li, H., Tan, L., 2015. Effects of salinity on the transformation of heavy metals in tropical estuary wetland soil. Chem. Ecol. 31, 186–198.

Curtin, D., Trolove, S., 2013. Predicting pH buffering capacity of New Zealand soils from organic matter content and mineral characteristics. Soil Res. 51, 494–502.

Ding, S., Han, C., Wang, Y., Yao, L., Wang, Y., Xu, D., Sun, Q., Williams, P.N., Zhang, C., 2015. In situ, high-resolution imaging of labile phosphorus in sediments of a large eutrophic lake. Water Res. 74, 100–109.

de Livera, J., McLaughlin, M.J., Hettiarachchi, G.M., Kirby, J.K., Beak, D.G., 2011. Cadmium solubility in paddy soils: effects of soil oxidation, metal sulfides and competitive ions. Sci. Total Environ. 409, 1489–1497.

Esfandiar, N., Suri, R., McKenzie, E.R., 2022. Competitive sorption of Cd, Cr, Cu, Ni, Pb and Zn from stormwater runoff by five low-cost sorbents; Effects of co-contaminants, humic acid, salinity and pH. J. Hazard Mater. 423, 126938.

Fulda, B., Voegelin, A., Kretzschmar, R., 2013. Redox-controlled changes in cadmium solubility and solid-phase speciation in a paddy soil as affected by reducible sulfate and copper. Environ. Sci. Technol. 47, 12775–12783.

Furuya, M., Hashimoto, Y., Yamaguchi, N., 2016. Time-course changes in speciation and solubility of cadmium in reduced and oxidized paddy soils. Soil Sci. Soc. Am. J. 80, 870–877.

Grybos, M., Davranche, M., Gruau, G., Petitjean, P., Pedrot, M., 2009. Increasing pH drives organic matter solubilization from wetland soils under reducing condition. Geoderma 154, 13–19.
Guo, S.H., Liu, Z.L., Li, Q.S., Yang, P., Wang, L.L., He, B.Y., Xu, Z.M., Ye, J.S., Zeng, E.Y., 2016. Leaching heavy metals from the surface soil of reclaimed tidal flat by alternating seawater inundation and air drying. Chemosphere 157, 262–270.
He, L., Shan, J., Zhao, X., Wang, S., Yan, X., 2019. Variable responses of nitrification and denitrification in a paddy soil to long-term biochar amendment and short-term biochar addition. Chemosphere 234, 558–567.
He, S., He, Z., Yang, X., Stoffella, P.J., Baligar, V.C., 2015. Soil biogeochemistry, plant physiology, and phytoremediation of cadmium-contaminated soils. Adv. Agron. 134, 135–225.
Heron, G., Crouzet, C., Bourg, A.C.M., Christensen, T.H., 1994. Speciation of Fe(II) and Fe(III) in contaminated aquifer sediments using chemical extraction techniques. Environ. Sci. Technol. 28, 1698–1705.
Hu, Y., Cheng, H., Tao, S., 2016. The Challenges and solutions for cadmium-contaminated rice in China: a critical review. Environ. Int. 92–93, 515–532.
Hussain, B., Ashraf, M.N., Shafeeq ur, R., Abbas, A., Li, J., Farooq, M., 2021. Cadmium stress in paddy fields: effects of soil conditions and remediation strategies. Sci. Total Environ. 754, 142188.
Inahara, M., Ogawa, Y., Azuma, H., 2007. Countermeasure by means of flooding in latter growth stage to restrain cadmium uptake by lowland rice [Oryza sativa]. Jpn. J. Soil Sci. Plant Nutr. 78, 149–155.
Jiang, J., Wang, Y.P., Yu, M., Cao, N., Yan, J., 2018. Soil organic matter is important for acid buffering and reducing aluminum leaching from acidic forest soils. Chem. Geol. 501, 86–94.
Johnson, K.A., Simpson, Z.B., Blom, T., 2009. Global Kinetic Explorer: a new computer program for dynamic simulation and fitting of kinetic data. Anal. Biochem. 387, 20–29.
Kögel-Knabner, I., Amelung, W., Cao, Z., Fiedler, S., Frenzel, P., Jahn, R., Kalbitz, K., Koelbl, A., Schloter, M., 2010. Biogeochemistry of paddy soils. Geoderma 157, 1–14.
Krishnamurti, G.S.R., Naidu, R., 2003. Solid-solution equilibria of cadmium in soils. Geoderma 113, 17–30.
Lambrechts, T., Couder, E., Bernal, M.P., Faz, A., Iserentant, A., Lutts, S., 2011. Assessment of heavy metal bioavailability in contaminated soils from a former mining area (La Union, Spain) using a rhizospheric test. Water Air Soil Pollut. 217, 333–346.
Li, S., Wang, M., Zhao, Z., Ma, C., Chen, S., 2018. Adsorption and desorption of Cd by soil amendment: mechanisms and environmental implications in field-soil remediation. Sustainability 10, 2337.
Liu, P., Wang, P., Lu, Y., Ding, Y., Lu, G., Dang, Z., Shi, Z., 2019. Modeling kinetics of heavy metal release from field-contaminated soils: roles of soil adsorbents and binding sites. Chem. Geol. 506, 187–196.
Liu, Y., Alessi, D.S., Flynn, S.L., Alam, M.S., Hao, W., Gingras, M., Zhao, H., Konhauser, K.O., 2018. Acid-base properties of kaolinite, montmorillonite and illite at marine ionic strength. Chem. Geol. 483, 191–200.
Loganathan, P., Vigneswaran, S., Kandasamy, J., Naidu, R., 2012. Cadmium sorption and desorption in soils: a review. Crit. Rev. Environ. Sci. Technol. 42, 489–533.
López-Chuken, U.J., Young, S.D., 2010. Modelling sulphate-enhanced cadmium uptake by *Zea mays* from nutrient solution under conditions of constant free Cd^{2+} ion activity. J. Environ. Sci. 22, 1080–1085.
Lu, R.K., 2000. Soil and Agro-Chemistry Analysis Methods. China Agricultural Science and Tech-nology Press, Beijing.
Lu, S.G., Malik, Z., Chen, D.P., Wu, C.F., 2014. Porosity and pore size distribution of Ultisols and correlations to soil iron oxides. Catena 123, 79–87.
Oporto, C., Smolders, E., Degryse, F., Verheyen, L., Vandecasteele, C., 2009. DGT-measured fluxes explain the chloride-enhanced cadmium uptake by plants at low but not at high Cd supply. Plant Soil 318, 127–135.
Ondrasek, G., 2014. Water Scarcity and Water Stress in Agriculture. Physiological Mechanisms and Adaptation Strategies in Plants under Changing Environment. Springer, pp. 75–96.
Ondrasek, G., Romic, D., Rengel, Z., 2020. Interactions of humates and chlorides with cadmium drive soil cadmium chemistry and uptake by radish cultivars. Sci. Total Environ. 702, 134887.
Ondrasek, G., Rengel, Z., Maurovic, N., Kondres, N., Filipovic, V., Savic, R., Blagojevic, B., Tanaskovik, V., Gergichevich, C.M., Romic, D., 2021. Growth and element uptake by salt-sensitive crops under combined NaCl and Cd stresses. Plants-Basel 10, 1202.
Ondrasek, G., Badovinac, I.J., Peter, R., Petravic, M., Macan, J., Rengel, Z., 2022. Humates and chlorides synergistically increase Cd phytoaccumulation in strawberry fruits, heightening health risk from Cd in human diet. Exposure and Health 14, 393–410.
Pan, Y., Koopmans, G.F., Bonten, L.T.C., Song, J., Luo, Y., Temminghoff, E.J.M., Comans, R.N.J., 2016. Temporal variability in trace metal solubility in a paddy soil not reflected in uptake by rice (*Oryza sativa* L.). Environ. Geochem. Health 38, 1355–1372.
Pandey, A., Kumar, A., Pandey, D., Thongbam, P., 2014. Rice quality under water stress. Indian J. Adv. Plant Res 1, 23–26.
Puy, J., Galceran, J., Cruz-Gonzalez, S., David, C.A., Uribe, R., Lin, C., Zhang, H., Davison, W., 2014. Measurement of metals using DGT: impact of ionic strength and kinetics of dissociation of complexes in the resin domain. Anal. Chem. 86, 7740–7748.
Reddy, I.N.B.L., Kim, B.K., Yoon, I.S., Kim, K.H., Kwon, T.R., 2017. Salt tolerance in rice: focus on mechanisms and approaches. Rice Sci. 24, 123–144.
Smolders, E., McLaughlin, M.J., 1996. Chloride increases cadmium uptake in Swiss chard in a resin-buffered nutrient solution. Soil Sci. Soc. Am. J. 60, 1443–1447.
Song, X., Wang, P., Van Zwieten, L., Bolan, N., Wang, H., Li, X., Cheng, K., Yang, Y., Wang, M., Liu, T., 2022. Towards a better understanding of the role of Fe cycling in soil for carbon stabilization and degradation. Carbon Research 1, 1–16.
Steinmuller, H.E., Chambers, L.G., 2018. Can saltwater intrusion accelerate nutrient export fromfreshwater wetland soils? An experimental approach. Soil Sci. Soc. Am. J. 82, 283–292.
Suda, A., Makino, T., 2016. Functional effects of manganese and iron oxides on the dynamics of trace elements in soils with a special focus on arsenic and cadmium: a review. Geoderma 270, 68–75.
Tanji, K.K., Kielen, N.C., 2002. Agricultural Drainage Water Management in Arid and Semi-arid Areas. Fao irrigation drainage paper rome.
Tavakkoli, E., Rengasamy, P., Smith, E., McDonald, G.K., 2015. The effect of cation-anion interactions on soil pH and solubility of organic carbon. Eur. J. Soil Sci. 66, 1054–1062.
Thanh, N.V., Bharali, B., 2019. Salinity stress on rice (*Oryza sativa* L.) crop and its amelioration. Pharmacogn. Phytochem 8, 1435–1441.
Tian, L., Shi, Z., Lu, Y., Dohnalkova, A.C., Lin, Z., Dang, Z., 2017. Kinetics of cation and oxyanion adsorption and desorption on ferrihydrite: roles of ferrihydrite binding sites and a unified model. Environ. Sci. Technol. 51, 10605–10614.
Tully, K., Gedan, K., Epanchin Niell, R., Strong, A., Bernhardt, E.S., Bendor, T., Mitchell, M., Kominoski, J., Jordan, T.E., Neubauer, S.C., Weston, N.B., 2019. The invisible flood: the chemistry, ecology, and social implications of coastal saltwater intrusion. Bioscience 69, 368–378.
Viet, N., Bharali, B., 2019. Salinity stress on rice (*Oryza sativa* L.) crop and its amelioration. J. Pharmacogn. Phytochem. 8, 1435–1441.
Wan, Y., Huang, Q., Camara, A.Y., Wang, Q., Li, H., 2019. Water management impacts on the solubility of Cd, Pb, As, and Cr and their uptake by rice in two contaminated paddy soils. Chemosphere 228, 360–369.
Wang, J., Wang, P.M., Gu, Y., Kopittke, P.M., Zhao, F.J., Wang, P., 2019. Iron-manganese (oxyhydro)oxides, rather than oxidation of sulfides, determine mobilization of Cd during soil drainage in paddy soil systems. Environ. Sci. Technol. 53, 2500–2508.
Wang, R.H., Zhu, X.F., Qian, W., Zhao, M.H., Xu, R.K., Yu, Y.C., 2016a. Adsorption of Cd (II) by two variable-charge soils in the presence of pectin. Environ. Sci. Pollut. Control Ser. 23, 12976–12982.
Wang, T., Liu, W., Xiong, L., Xu, N., Ni, J., 2013. Influence of pH, ionic strength and humic acid on competitive adsorption of Pb(II), Cd(II) and Cr(III) onto titanate nanotubes. Chem. Eng. J. 215, 366–374.
Wang, Y., Ding, S., Gong, M., Xu, S., Xu, W., Zhang, C., 2016b. Diffusion characteristics of agarose hydrogel used in diffusive gradients in thin films for measurements of cations and anions. Anal. Chim. Acta 945, 47–56.
Weggler, K., McLaughlin, M.J., Graham, R.D., 2004. Effect of chloride in soil solution on the plant availability of biosolid-borne cadmium. J. Environ. Qual. 33, 496–504.
Xiao, W., Ye, X., Zhu, Z., Zhang, Q., Zhao, S., Chen, D., Fang, X., Gao, N., Hu, J., 2020. Evaluation of cadmium (Cd) transfer from paddy soil to rice (*Oryza sativa* L.) using DGT in comparison with conventional chemical methods: derivation of models to predict Cd accumulation in rice grains. Environ. Sci. Pollut. Control Ser. 27, 14953–14962.
Xu, R.K., Zhao, A.Z., Yuan, J.H., Jiang, J., 2012. pH buffering capacity of acid soils from tropical and subtropical regions of China as influenced by incorporation of crop straw biochars. J. Soils Sediments 12, 494–502.
Yang, Y., Peng, Y., Wang, Y., Li, F., Liu, T., 2019a. Surface complexation model of Cd in paddy soil and its validation with bioavailability (in Chinese). Chin. Sci. Bull. 64, 3449–3457.
Yang, X., Lin, R., Zhang, W., Xu, Y., Wei, X., Zhuo, C., Qin, J., Li, H., 2019b. Comparison of Cd subcellular distribution and Cd detoxification between low/high Cd-accumulative rice cultivars and sea rice. Ecotoxicol. Environ. Saf. 185, 109698.
Yang, Y., Wang, Y., Peng, Y., Cheng, P., Li, F., Liu, T., 2020. Acid-base buffering characteristics of non-calcareous soils: correlation with physicochemical properties and surface complexation constants. Geoderma 360, 114005.
Yang, Y., Yuan, X., Chi, W., Wang, P., Hu, S., Li, F., Li, X., Liu, T., Sun, Y., Qin, H., 2021. Modelling evaluation of key cadmium transformation processes in acid paddy soil under alternating redox conditions. Chem. Geol. 581, 120409.
Yang, X., Li, J., Zheng, Y., Li, H., Qiu, R., 2022. Salinity elevates Cd bioaccumulation of sea rice cultured under co-exposure of cadmium and salt. J. Environ. Sci. 126, 602–611.
Yu, H.Y., Li, F.B., Liu, C.S., Huang, W., Liu, T.X., Yu, W.M., 2016. Iron redox cycling coupled to transformation and immobilization of heavy metals: implications for paddy rice safety in the Red Soil of South China. Adv. Agron. 137, 279–317.
Yuan, C., Li, F., Cao, W., Yang, Z., Hu, M., Sun, W., 2019. Cadmium solubility in paddy soil amended with organic matter, sulfate, and iron oxide in alternative watering conditions. J. Hazard Mater. 378, 120672.
Zhang, H., Davison, W., 1995. Performance characteristics of diffusion gradients in thin films for the in situ measurement of trace metals in aqueous solution. Anal. Chem. 67, 3391–3400.
Zhang, W., Li, X., Liu, T., Li, F., 2012. Enhanced nitrate reduction and current generation by Bacillus sp in the presence of iron oxides. J. Soils Sediments 12, 354–365.
Zhang, X., Zeng, S., Chen, S., Ma, Y., 2018. Change of the extractability of cadmium added to different soils: aging effect and modeling. Sustainability 10, 885.
Zhang, K., Yang, Y., Chi, W., Chen, G., Du, Y., Hu, S., Li, F., Liu, T., 2023. Chromium transformation driven by iron redox cycling in basalt-derived paddy soil with high geological background values. J. Environ. Sci. 125, 470–479.